Detection of Anomalous Elements, X-Ray, and Excess Heat in a D₂-Pd System and Its Interpretation by the Electron-Induced Nuclear Reaction Model

Yasuhiro Iwamura, Takehiko Itoh, Nobuaki Gotoh & Ichiro Toyoda

Published online: 09 May 2017.

Submit your article to this journal

View related articles

Citing articles: 3 View citing articles

DETECTION OF ANOMALOUS ELEMENTS, X-RAY, AND EXCESS HEAT IN A D$_2$-Pd SYSTEM AND ITS INTERPRETATION BY THE ELECTRON-INDUCED NUCLEAR REACTION MODEL

YASUHIRO IWAMURA,* TAKEHIKO ITOH, NOBUAKI GOTOH, and ICHIRO TOYODA *Advanced Technology Research Center*
Mitsubishi Heavy Industries, Ltd., 1-8-1, Sachiura, Kanazawa-ku
Yokohama 236, Japan

A new type of experimental apparatus is developed to induce continuous diffusion of deuterium, in which an electrochemical cell for calorimetry and a vacuum chamber for nuclear measurement are divided by a Pd sheet. Continuous X rays ranging from 10 to 100 keV and neutron and excess heat production are observed using the apparatus. Titanium atoms are detected on the surface where deuterium atoms pass through on Pd cathodes after electrolysis. Quantitative discussion shows that the detected Ti atoms cannot be explained by contamination. An electron-induced nuclear reaction (EINR) model for explaining the obtained experimental results is introduced. Experimental support of the EINR model is demonstrated by using multilayer cathodes, in which a layer containing Ca is placed at the near surface of Pd, based on the EINR model.

I. INTRODUCTION

Almost 8 yr has passed since the announcement of "cold fusion" by Fleischmann and Pons.[1] Because of the possibility of cold fusion being a new energy technology, considerable effort has been expended to confirm Fleischmann and Pons's experimental results, i.e., that nuclear reactions are electrochemically induced in a D$_2$-Pd

system. However, the nature and reaction mechanism still remain uncertain, probably because of the lack of experimental reproducibility or the long experimental time necessary to observe cold fusion phenomena.

Beginning in 1993, we have researched cold fusion to investigate its potentiality as a new energy source. At first, we performed gas-loading experiments, in which deuterium-tritium (D-T) gas and neutron emission were observed.[2] We showed that the diffusion process of deuterium, in addition to a high D/Pd ratio, is an important factor for causing nuclear reactions. Based on these experimental results, we developed a new experimental apparatus for continuous diffusion of deuterium.[3–6]

In this paper, we explain our new type of experimental apparatus and the results of simultaneous measurement of excess heat and nuclear products. Anomalous and unexpected elements detected on Pd cathodes after experiments are also described. In Sec. IV, we propose the hypothetical Electron-Induced Nuclear Reaction (EINR) model to explain and investigate cold fusion. Experimental support of the model using multilayer cathodes, which have been designed based on the EINR model, is described.

II. EXPERIMENTAL METHOD

II.A. Experimental System

A high D/Pd ratio is recognized as one of the necessary conditions to induce nuclear reactions. However, it is not sufficient. The other conditions still remain unclarified at present. As mentioned earlier, the diffusion
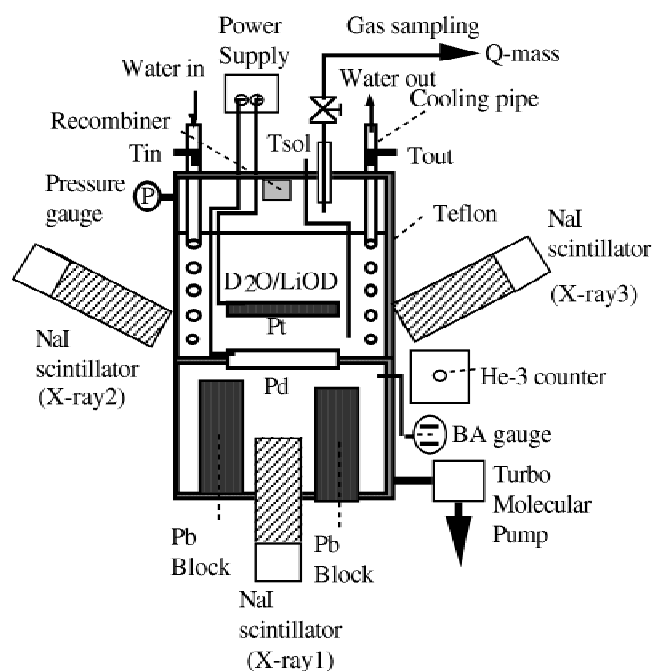
---

*E-mail: iwamura@atrc.mhi.co.jp

Fig. 1. Experimental apparatus.

process of deuterium atoms is important. Therefore, if we kept the D_2-Pd system under *certain appropriate conditions* relating to the D/Pd and diffusion process, it might be possible to cause nuclear reactions at all times.

The basic idea of our new apparatus is that we might make nuclear reactions occur always by a method that makes a continuous flow of deuterium and controls the diffusion process of deuterium.

Figure 1 shows a cross-sectional view of the continuous diffusion experimental apparatus.[6] An electrolyte of $1 M$ LiOD/D_2O and a vacuum chamber are separated by a Pd plate with an O-ring gasket.[a] Deuterium atoms are loaded by electrochemical potential into one side of the Pd sample and released from the other side. A continuous flow of deuterium atoms exits from the electrochemical side. With this composition, it is possible to control the state of diffusion of deuterium by applied current or pressure of the vacuum side.

Excess heat is estimated by the flow calorimetry method.[b] The electrolyte side of the apparatus consists of a Pd plate cathode ($25 \times 25 \times 1$ mm),[c] a circular Pt mesh anode (ϕ 0.5 mm),[d] a recombiner, and a cooling pipe to measure excess heat generation.

Pressures in the upper part of the electrolyte and vacuum chamber are monitored by a pressure gauge and a BA

gauge, respectively. At the beginning of electrolysis, Ar gas is filled up at 1 atm in the upper space of the electrolyte.

The recombiner is prepared by electroplating the Pt mesh in a H_2PtCl_6 solution. In this apparatus, an increase of pressure at the upper part of the electrolyte corresponds to absorbed deuterium because D_2 and O_2 are generated by electrolysis, and D_2:$O_2 = 2$:1. If some D_2 is absorbed into Pd, then all the remaining D_2 is recombined by O_2 gas on the recombiner on the condition that recombiner efficiency is 100%. The O_2 gas, which has no partner for recombination, remains in the upper part of the electrolyte. Therefore, two times the amount of the remaining O_2 corresponds to the amount of absorbed D_2.

Recombiner efficiency is calculated by analyzing the D_2 and O_2 gases in the upper part of the electrolyte using a quadrupole mass spectrometer.[e] Furthermore, the temperature of the recombiner is always monitored to make sure that the recombiner works. We confirm that the recombiner works by temperature and gas analysis. The usual recombiner efficiency that we measured was >99%.

The cooling pipe is electroplated with Au (10 μm thick) because Au is resistant to alkaline solution and good thermal conductivity. The flow rate of the coolant (pure water) is always measured at two points: at the inlet and outlet sides. Furthermore, the flow rate is measured by a mass cylinder.

Two thermocouples each are provided to measure the inlet and outlet temperatures of the water. The solution, gas, recombiner, and environmental temperatures are measured, and the consistency among these temperatures is always checked.

The cell of the electrolyte side of the apparatus is made of Teflon, which is stable material for an alkaline solution. All experimental parts such as the electric wires in the electrolyte side are coated with sprayed Teflon.

The apparatus is equipped with three NaI scintillation counters[f] for X-ray spectroscopy and a ^{3}He neutron detector.[g] The X-ray 1 detector, located in the vacuum chamber, is surrounded by a Pb cylinder (thickness: 2.5 cm) to reduce background X rays. X-ray spectroscopy and the counting system consist of preamplifiers,[h] amplifier and single-channel analyzers,[i] counters,[j] and multichannel analyzers.[k] As to neutron counting, we use a preamplifier,[l] an amplifier and single-channel analyzer,[m] and a counter.[n]

---

[a]By KALREZ.

[b]Heavy water (up to 99.9%) and LiOD (up to 99%) are provided by ISOTEC, Inc.

[c]99.9% Tanaka Kikinzoku Kogyo K.K.

[d]99.98% Nilaco Company.

---

[e]AQA-360, ANELVA.

[f]Bicron: 1.5XM1/2B.

[g]Reuter-Stokes: RS-0806-207.

[h]EG&G Ortec: 276.

[i]EG&G Ortec: 590A.

[j]EG&G Ortec: 997.

[k]SEIKO EG&G: MCA4100, 4200.

[l]EG&G Ortec: 142PC.

[m]EG&G Ortec: 590A.

[n]EG&G Ortec: 997.

The experimental data except for the X-ray energy spectrum are acquired every 20 s by a data logger and a personal computer. The energy spectrum of X rays is obtained every 6 h. The apparatus and measuring systems are located in a clean room, where the temperature and humidity are always controlled at constant levels ($23 \pm 1°C$, $40 \pm 5\%$). All these electrical instruments are supplied by an isolated power source to prevent electric noise from the outside of the clean room.

II.B. Palladium Preparation

Palladium preparation is one of the most important factors to observe anomalous nuclear reactions. It is believed that the lack of reproducibility is related to the variation of the metallurgical conditions of the Pd metal.

The procedure for sample preparation is as follows. Palladium plates were washed with acetone and annealed under vacuum conditions ($<10^{-7}$Torr) at 900°C for 10 h. The samples were cooled down to room temperature in the furnace and washed with aqua regia(D_2O) to remove impurities on the surface of the Pd samples. After that, some samples were covered with Al or MgO by Ar ion beam sputtering, some samples were electroplated by Cu or Pt, and the others had no films. The aim of the surface modification is to reduce the rate of deuterium gas release from the vacuum side of the Pd.

II.C. Data Analysis

The following procedure is used to estimate D/Pd. The equation of state for the upper part of the electrolyte side is expressed as

$$p_{O_2}V_{cell} = N_{O_2}\kappa T_{cell} \ , \tag{1}$$

where *cell* denotes the upper part of the electrolyte side and κ is the Boltzmann constant. The number of deuterium atoms absorbed into the Pd is given by

$$N_{D_{in}} = 2N_{D_2} = 4N_{O_2} = \frac{4V_{cell}p_{O_2}}{\kappa T_{cell}} \ . \tag{2}$$

As the vacuum chamber is evacuated by the pumping speed of S, an equation of mass balance is obtained as follows:

$$\frac{d}{dt}(N_{vac}\kappa T_{vac}) = V_{vac}\dot{p}_{vac} + P_{vac}S \ , \tag{3}$$

where *vac* denotes the vacuum side. The major component in the vacuum chamber is D_2 gas. Therefore, the time derivative of the number of deuterium atoms is given by

$$\dot{N}_{D_{out}} = 2\frac{V_{vac}\dot{p}_{vac} + p_{vac}S}{\kappa T_{vac}} \ . \tag{4}$$

Combining Eqs. (2) and (4), we obtain the following equation:

$$\text{D/Pd} = \frac{M_{Pd}}{\omega_{Pd}N_{AB}}\left(\frac{4V_{cell}p_{O_2}}{\kappa T_{cell}} - 2\int_{t_0}^{t}\frac{V_{vac}\dot{p}_{vac} + p_{vac}S}{\kappa T_{vac}}\,dt\right) \ , \tag{5}$$

where

N_{AB} = Avogadro number

m_{Pd} = mass number of Pd

ω_{Pd} = mass of the Pd sample

t_0 = time that D_2 gas begins to release out.

Next, we describe the excess heat analysis. In the following analysis, we consider only the steady state.

The heat balance equation of the apparatus is expressed as

$$P_{ex} + P_{in} - P_{out} - P_{diss} - \Delta\dot{H}_{gas} + \Delta\dot{H}_{abs} - \Delta\dot{H}_{des} = 0 \ , \tag{6}$$

where

ex = excess

in = input

out = output

$diss$ = dissipation

gas = gas release

abs = absorption

des = desorption.

The terms of the gas release, absorption, and desorption of deuterium are negligible if we use actual experimental parameters. For example, the enthalpy change by deuterium gas release is calculated as follows:

$$\Delta H_{gas} = \tfrac{7}{2}N_{D_2}\kappa T_{D_2} = \tfrac{7}{2}P_{vac}V_{vac}$$

$$\therefore \Delta\dot{H}_{gas} = \tfrac{7}{2}(\dot{P}_{vac}V_{vac} + P_{vac}\dot{V}_{vac}) \approx \tfrac{7}{2}P_{vac}S$$

$$P_{vac} \approx 1 \times 10^{-2} \ (\text{Pa})$$

$$S = 50 \ (\ell/s)$$

$$\therefore \Delta\dot{H}_{gas} \approx 2 \times 10^{-3} \ (\text{W}) \ ,$$

where 2 mW is negligible because the input power is $\sim$20 W. Therefore, excess heat is calculated by

$$P_{ex} = \dot{m}_w c_w(T_{out} - T_{in}) - IV + \int_A h(T_{sol} - T_{room})\,dA \ , \tag{7}$$

where

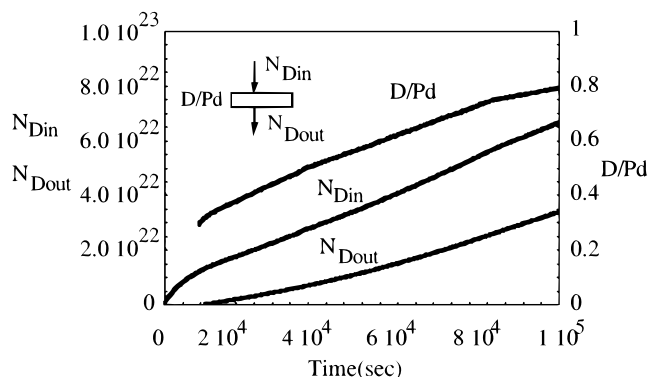IV = input power

m_w = mass of the water

Fig. 2. D/Pd analysis.

cw = mass of the specific heat

h = heat transfer coefficient

A = whole surface of the apparatus.

The term of dissipated heat from the apparatus is estimated by the Pd/H$_2$O system, in which we assume no excess heat.

III. RESULTS AND DISCUSSION

III.A. Behavior of Deuterium in Pd

Figure 2 shows an example of D/Pd analysis. In this case, the sample has no surface film. Because the deuterium atoms absorbed on the surface of the electrolyte side of the Pd do not reach the opposite surface, deuterium gas is not released at the early period of the experiment. D/Pd increases gradually to 0.8 by 1×10^5 s. These results indicate that D/Pd reaches $\sim$0.8 for even the Pd sample without a surface barrier on the vacuum side of it.

The variation of the deuterium behavior depending on the Pd samples is shown in Fig. 3. The pressure (electrolyte) lines, which mean the pressures in the upper part of the electrolyte side, correspond to the quantity of deuterium in the Pd [Eq. (2)]. The pressure (vacuum) lines mean the pressures in the vacuum side, which are related to the time derivatives of the number of released deuterium atoms [Eq. (4)].

These samples, EV29 and EV34, are prepared by the same procedure; they are derived from the same lot, and the method of annealing and etching is all the same. However, it is easy to see that the absorption and desorption of deuterium are entirely different, which suggests that the absorption and desorption behavior of deuterium is greatly influenced by unspecified factors, i.e., metallurgical conditions such as impurity and defects in Pd.

III.B. X-Ray and Neutron Emission

An example of a long period of X-ray emission and its energy spectrum is illustrated in Fig. 4. This sample has thin Al film (400 Å). Figure 4a indicates the time variation of X-ray 1 (see Fig. 1) located in the vacuum chamber. The X-ray 1 count rate reaches more than 10 times that of the background. The X-ray energy for the counting ranges from 18.8 to 383 keV. A storage digital oscilloscope showed that the shapes of the observed electronic signals were not different from the shapes of true X-ray signals by ^{241}Am. In this case, the detectors of X-rays 2 and 3 were not installed.

We can see that X-ray emission lasts for a long period, i.e., >1 day, which successfully exemplifies that we could make long-term continuous nuclear reactions occur in the D$_2$-Pd system.

Energy spectra for the X-ray emission (foreground) and background are plotted in Fig. 4b. Figure 4c shows the X-ray energy spectrum with the background subtracted out. The X-ray energy is distributed from $\sim$12 to 100 keV continuously as shown in Fig. 4c. Note that a characteristic X-ray (K-α,β) of Pd ($\sim$21 keV) was not
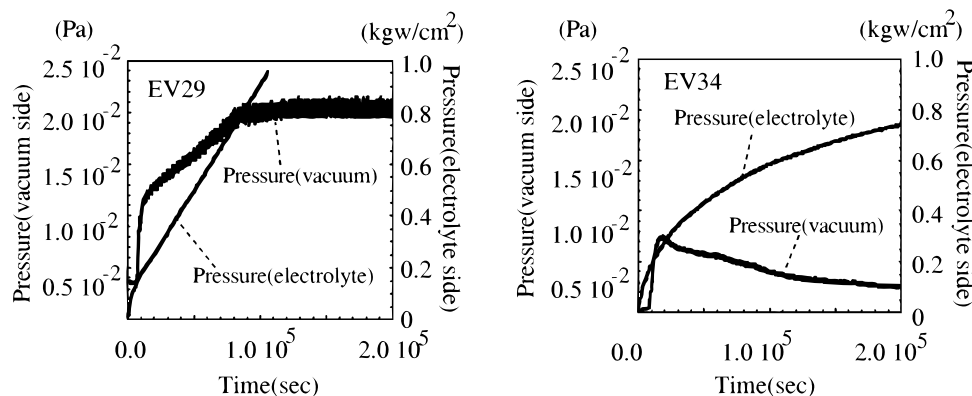

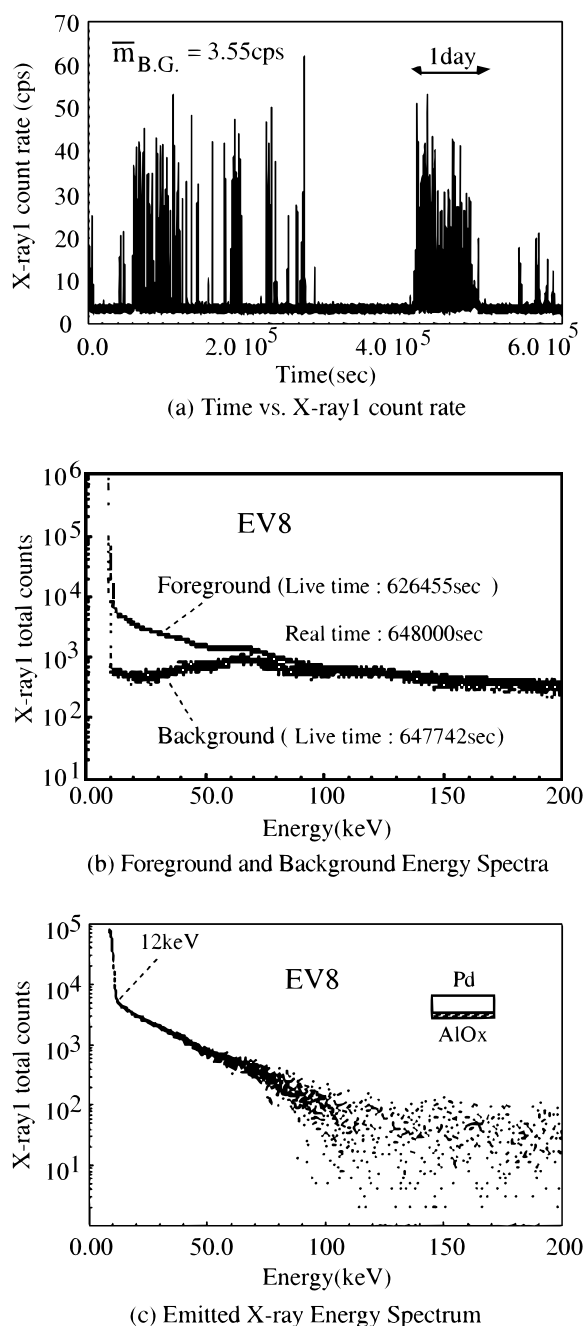Fig. 3. Variation of absorption and desorption of deuterium.

(a) Time vs. X-ray1 count rate

(b) Foreground and Background Energy Spectra

(c) Emitted X-ray Energy Spectrum

Fig. 4. Long-term X-ray emission and its energy spectrum.

Fig. 5. Simultaneous detection by upper-side X-ray detectors.

Fig. 6. Correlation between neutron and X-ray emission.

observed. One may suppose that low-energy charged particles less than ~ 100 keV emitted and induced bremsstrahlung, for the low-energy charged particles have a small cross section for ionizing k-shell electrons of Pd.

The next example shows the simultaneous detection by the upper side of X-ray NaI counters (Fig. 5). The EV23 sample is electroplated with Cu. The coincidence of X-rays 2 and 3 is very good; on the other hand, the counts of X-ray 1 are almost equal to those of the back-
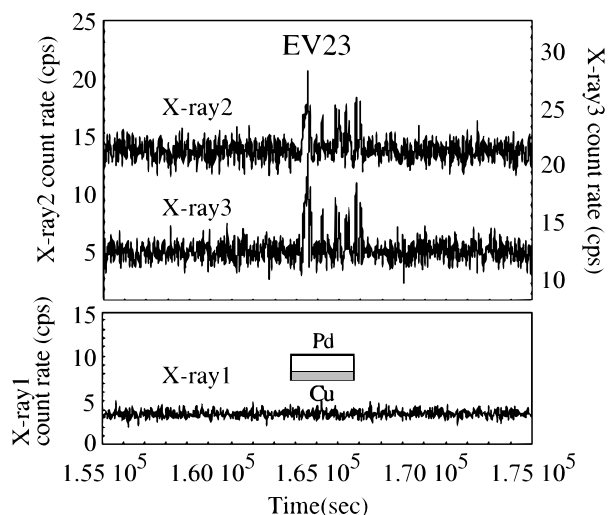
ground. We observed this type of X-ray emission many times (more than 20). In these cases, nuclear reactions must occur on the electrolyte side of the Pd. Because Pd is 1 mm thick, the reduction rate of X rays through the Pd is larger than that through the D_2O (4 cm).

Figure 6 shows the correlation between neutron and X-ray emission and indicates that the neutron and X-ray emission do not correspond. However, X-rays 2 and 3 are relatively high when the neutron bursts. It is considered that certain physical conditions that cause nuclear reactions were satisfied at about the time of the neutron bursts.

In our experiments, including gas release[2–4] and simple electrochemical experiments,[5] the probability of neutron emission is rather low, i.e., about a few percent or

so. On the other hand, the probability of X-ray emission is higher than that for neutrons.

Because of the weak correlation between the neutrons and X rays, in addition to the low reproducibility of neutron emission, it is certain that the neutrons and X rays are produced by different nuclear reactions.

III.C. Excess Heat

Figure 7 illustrates the correlation between excess heat and the other parameters. In this case (EV39), we use a Pd sample covered with thin MgO film. At low current, no excess heat can be seen. However, after making the applied current up to 3 A (current density : 1.5 A/cm^2), we can observe clear excess heat generation. The input power is ∼40 W when a current of 3 A is applied; therefore, excess heat is a few percent of the input power.

A comparison of the heat distribution between EV39 (excess heat generation) and EV40 (no excess heat) is shown in Fig. 8. In both cases, the other experimental conditions are the same except for the Pd sample treatment. Thin MgO film is formed on the vacuum side of EV39, and thin Fe film is formed on the electrolyte side of EV40. The thin Fe film was deposited on EV40 to prevent inducing nuclear reactions.

As described earlier, we obtained experimental data every 20 s; therefore, excess heat is calculated every 20 s. Excess heat is calculated by a temperature increase
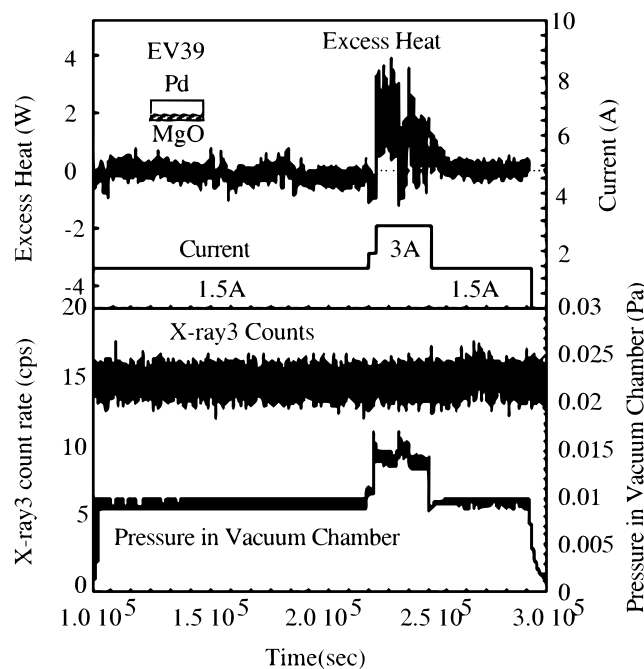

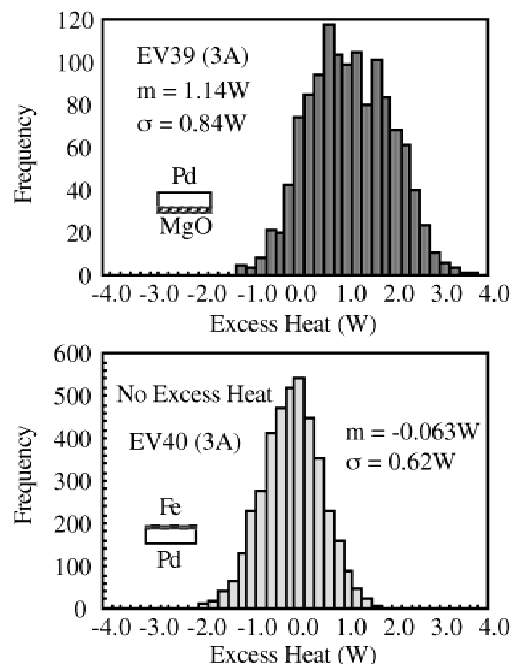Fig. 8. Excess heat distribution.

Fig. 7. Correlation between excess heat and the other parameters.

of the coolant, the flow rate of the coolant, and the input power, which fluctuate within some ranges. Even if there is no excess heat release, we observe fluctuations of excess heat within certain ranges. Negative excess heat derives from the fluctuation. We can see that the distribution of EV40 is similar to a Gaussian distribution, and the mean value is close to 0. The standard deviation of EV40 (0.62 W) can be regarded as the fluctuation of this experimental system. It is clear that the average value and the deviation of the excess heat of EV39 are larger than those of EV40. It supports the excess heat generation of EV39.

Up to now, we observed excess heat generation several times; however, we could not see any clear relations between excess heat generation and X-ray emission. If we assume a few-mega-electron-volt-energy release by an event, the excess heat obtained corresponds to the order of 10^{12} events/s. On the other hand, observed X-ray emissions range from 10^2 to 10^4 events/s (calibrated by an ^{241}Am source).

Judging from these results, we might consider that excess heat and X rays are generated by different nuclear reactions. In Ref. 5 we suggested that X rays and neutrons are generated by different reactions. It seems that various nuclear reactions occur and produce various nuclear ashes. However, we must conduct further investigations to conclude that there is a correlation between excess heat and nuclear products because it is not clear whether or not the energy range and the sensitivity of the detection of nuclear products are appropriate.

III.D. Detection of Anomalous Elements on Pd Electrode

The most anomalous feature of the phenomena in the D_2-Pd system is our detection of various elements that did not exist before electrolysis. In our experiments, we often detected the unexpected elements on Pd electrodes. As reported in Ref. 5, twice we detected Pb elements with characteristic X-ray emissions. Some elements can be explained by certain contamination processes; however, some elements cannot. There exist some elements that cannot be attributed to contamination. In the following, we adopt the detection of Ti.

Figure 9 shows the appearance of a Pd sample (EV27) after the experiments. Excess heat of ~ 1 W lasted for 1 day in the case of EV27, although X rays and neutrons were not detected. The total time of the experiment was 3.4×10^5 s, and the total applied charge was 4.0×10^5 C. The black circle on the electrolyte side (surface A) corresponds to the place through which the deuterium atoms went; it is the shape of the Pt anode. In most cases, we see similar black circles corresponding to the shape of the anode. However, the shades of the black circle are different every time, although the experimental conditions (i.e., kind of Pd sample, solution, applied current, etc.) are almost all the same.

Contrarily, the vacuum side of the Pd looks clean. Its appearance is the same as before the experiments, independent of the deuterium passage. The round shape on the surface is attributed to the O-ring gasket. The shape of the O-ring gasket is larger than that of the black circle

on the electrolyte side. All the vacuum sides of the Pd samples used in the experiments seem clean. In fact, we did not detect any elements by electron probe microanalysis (EPMA) except for Pd on the vacuum sides of the Pd electrodes.

Figures 10a, 10b, and 10c show the wavelength dispersive X-ray spectrometry (WDX) spectrum by EPMA for surfaces A, B, and C, respectively. We see that Ti, Ca, and O exist on surface A. Especially, the peak of Ti is clear. On the other hand, no element except Pd is detected on surfaces B and C.

A most important problem is answering where these elements come from. Of course, we did not add Ti to the electrolyte or the Pd and Pt electrodes. A second problem is whether or not the WDX spectrum is truly reliable. First we treat the second problem, and then we discuss the first problem.

Figure 11 shows the results of energy dispersive X-ray spectrometry (EDX) for surface A, where Ti, Ca, and O are detected by WDX. Only titanium is seen in the EDX spectrum because the sensitivity of EDX is lower than WDX. It is expected that the main elements are both Pd and Ti on the surface of the black circle of EV27.

Auger electron spectrometry (AES) is a method that detects Auger electrons with an electron probe, while detecting characteristic X rays in EPMA. We analyzed two points on surface A of EV27 by AES (PHI1670). One is on the thick Ti layer, and the other is on the thin layer; they can be observed through a microscope. In the following, we show the results of the thick layer.

surface A : Surface where deuterium atoms passed through

surface B : Surface where no deuterium atoms passed through

(a) Electrolyte side of palladium (EV27)   (b) Vacuum side of palladium (EV27)
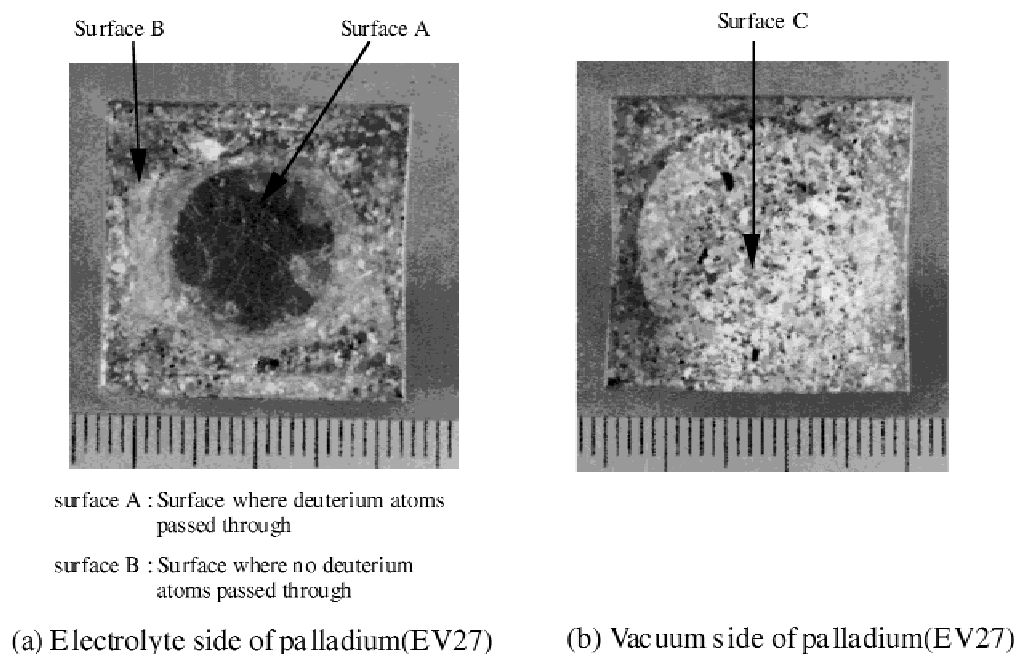
Fig. 9. (a) The electrolyte side of the Pd (EV27) and (b) the vacuum side of the Pd (EV27).
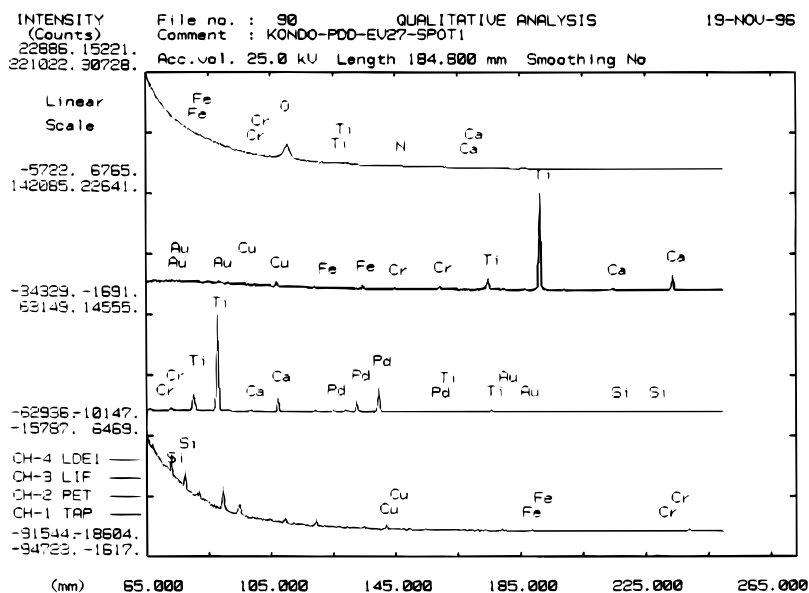
Fig. 10a. The WDX spectrum for the surface of the electrolyte side where deuterium atoms passed through (surface A of EV27).
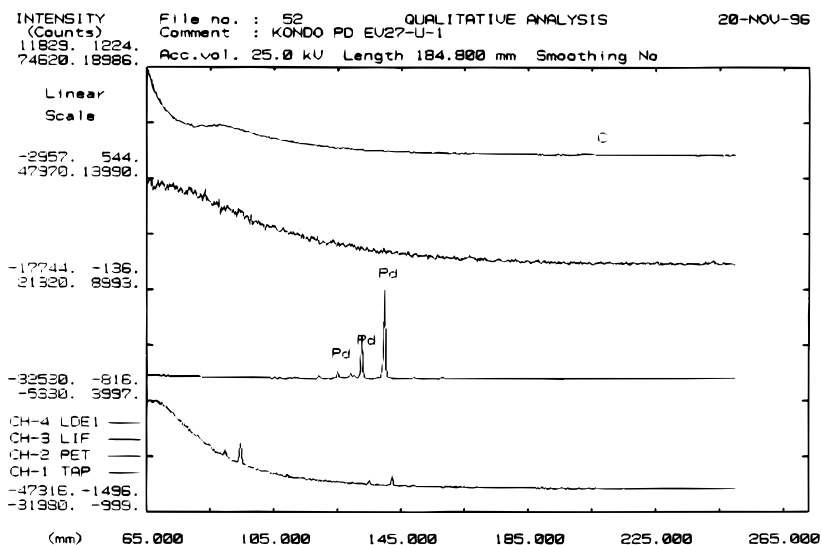

Fig. 10b. The WDX spectrum for the surface of the electrolyte side where no deuterium atoms passed through (surface B of EV27).

The AES differential spectrum is shown in Fig. 12. The sputter rate is 26 nm/min. Figure 12 is the AES spectrum when the sputter time is 30 min; it corresponds to an ~0.8-μm depth. Clear peaks of Ti and O can be seen.

Figure 13 shows the depth profile of surface A. It is made by summing up AES spectra for each sputter time. Titanium is the major element from the surface to 3 μm. The thickness of the Ti layer on the other point (the thin layer) is ~0.2 μm. Therefore, the thickness of the Ti layer

depends on the place on surface A. The Ti layer is thick: It can be called the "bulk" of Ti.

The last method of surface analysis is X-ray Photoelectron Spectrometry[o] (XPS). With XPS, photoelectron spectroscopy is performed with an X-ray probe. We applied XPS to surface A of EV27. The result of the XPS analysis after sputter (at a 4-nm depth) is plotted in

———————————————

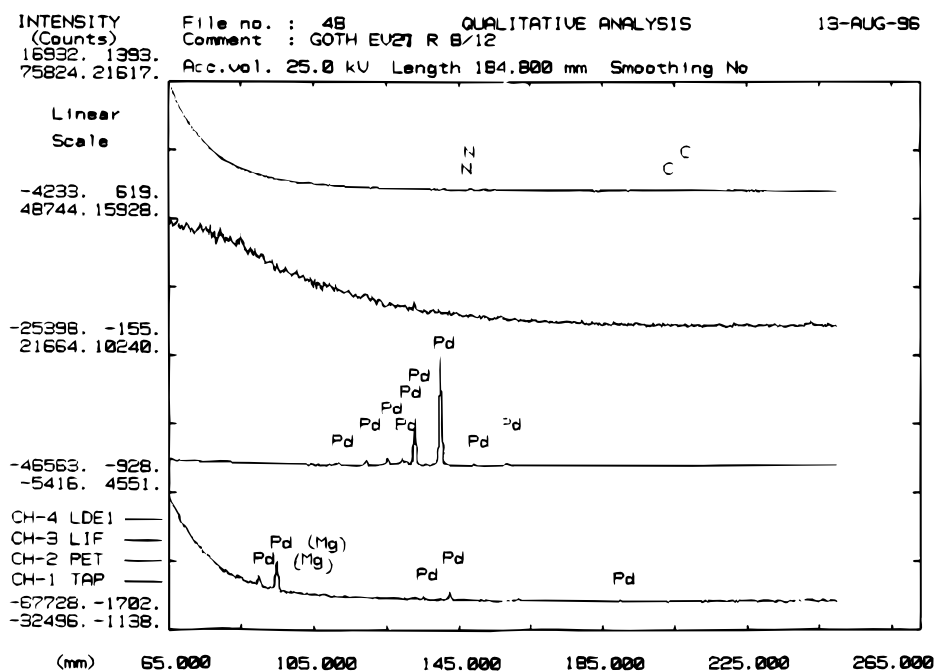[o]ESCA-300, SCIENTA and SEIKO Instruments.

Fig. 10c. The WDX spectrum for the surface of the vacuum side (surface C of EV27).

Fig. 14. The elements Ti, Ca, O, and Cu are detected, as shown in Fig. 14. The peak of Ti is clear.

According to the results by EPMA (WDX and EDX), AES, and XPS, Ti exists absolutely on surface A of EV27. Because Ca and O are also considered to be on surface A, we must ask where do these elements come from.

Table I[p] shows impurity analysis of an electrolyte, a Pt anode, and a Pd cathode. The LiOD/D_2O solution was kept for 3 days in the cell without electrolysis. The LiOD/D_2O solution and Pt were analyzed by inductively coupled plasma (ICP) mass spectroscopy (MS), ICP emission spectroscopy, and atomic photon absorption. Note that the LiOD solution and Pt wire contain small amounts of Ti. The maximum quantity of Ti contained in the LiOD/D_2O solution and Pt wire can be estimated at 3.3 μg.

The Pd sample was also analyzed by the same procedure, i.e., half the quantitative method.[q] Then, major and necessary impurities are reanalyzed by quantitative ICP-MS[r] at Takasogo Development and Research Center of Mitsubishi Heavy Industries, Ltd. Table II summarizes the results of the quantitative analysis.
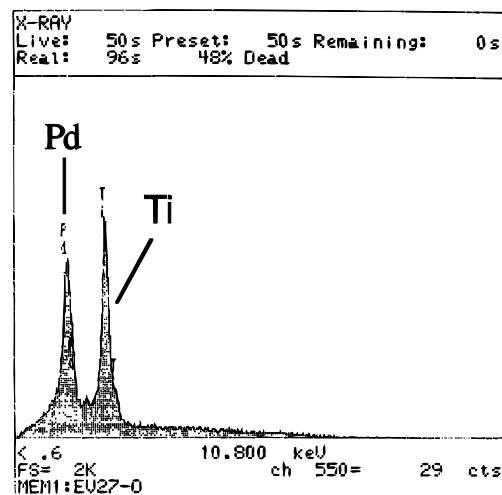
Fig. 11. The EDX spectrum for surface A.

An annealed Pd sample, a sample as received, EV27, EV34, and EV36 were analyzed. EV27 is the excess heat–producing sample on which Ti elements were detected. EV34 is the sample where X-ray and neutron emission was observed. For EV36, we did not observe any nuclear products: Any elements can be detected without Pd after electrolysis.

The quantity of Ti ranges from 2.2 to 2.5 μg/g except for EV27, as shown in Table II. The Ti concentration

---

[p]The Table I data were obtained by Toray Research Center, Inc. The LiOD solution was analyzed by SPQ9000 (SEIKO Instruments), SPS4000 (SEIKO Electronic Instruments), and Z8270 (Hitachi, Ltd.). The Pt wire was analyzed by SPQ6500 (SEIKO Instruments), SPS1200VR (SEIKO Electronic Instruments), and Z8270 (Hitachi, Ltd).

[q]By Toray Research Center, Inc.

[r]SPQ9000 (SEIKO Instruments).

AES Survey PC 5 Dec 96   Area: 2 Acquisition Time: 13.34 min

File: t4006 EV27-B

Scale Factor: 120.543 kc/s   Offset: -648.090 kc/s   Ep: 10.00 kV Ip: 0.0000 uA

Fig. 12. The differential Auger electron spectrum for surface A.

AES Depth Profile PC Alternating 5 Dec 96   Species: Au1 Region: 5 Area: 2 Sputter Time: 241.00 min
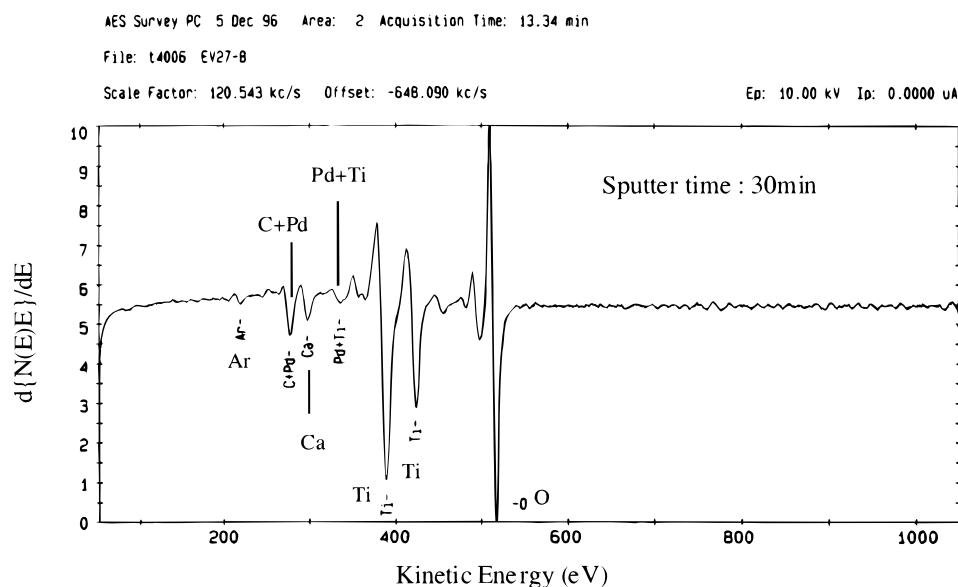
File: t4001 EV27-B

Scale Factor: 0.063 kc/s   Offset: 0.000 kc/s   Ep: 10.00 kV Ip: 0.0000 uA
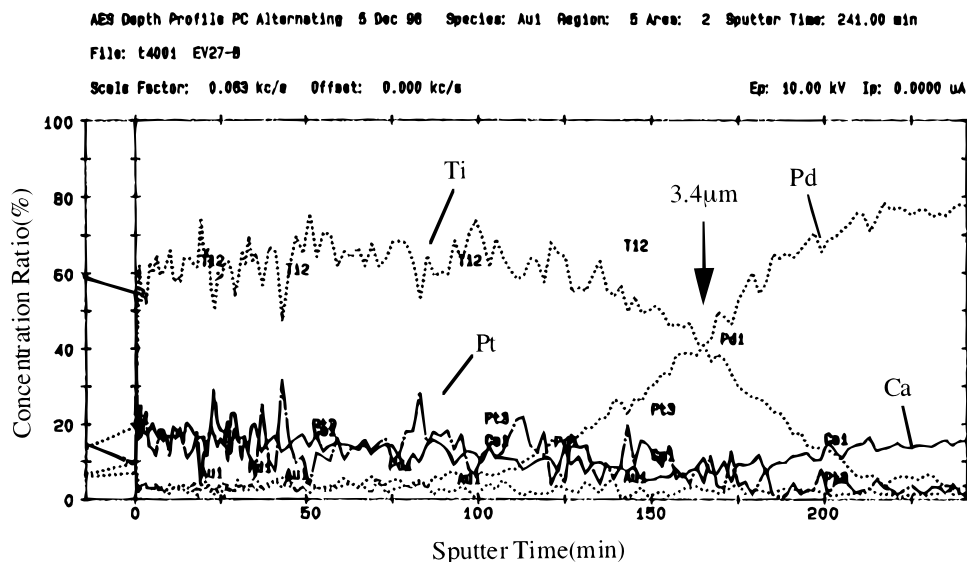
Fig. 13. The depth profile for surface A obtained by AES.

of EV27 is 18 μg/g, which is clearly high. These concentrations contain not only the surface but also the bulk of Pd: They are average values. We can estimate the increased mass of Ti on surface A of EV27. As the radius of the black circle is ~0.6 cm, then the estimated increased Ti mass is ~21 μg, which corresponds to 2.6 × 10^{17} atoms.

On the other hand, the mass of Ti in a whole Pd sample before electrolysis is ~19 μg (the Ti concentration is

2.5 μg/g, and the Pd size is 25 × 25 × 1 mm). Therefore, the maximum total mass of Ti in a Pd sample, LiOD/D_2O solution, and Pt wire is 22.3 μg, which is the same order of the increased mass of Ti on surface A.

It is very difficult to consider that only Ti elements were concentrated on the electrolyte surface, where deuterium atoms passed through by an ordinary physico-chemical process, while it is certain that an electric field was applied on the surface. Although concentrations of

Fig. 14. The XPS spectrum for surface A.

the Pd surface? We think that a selective concentration of Ti is unlikely.
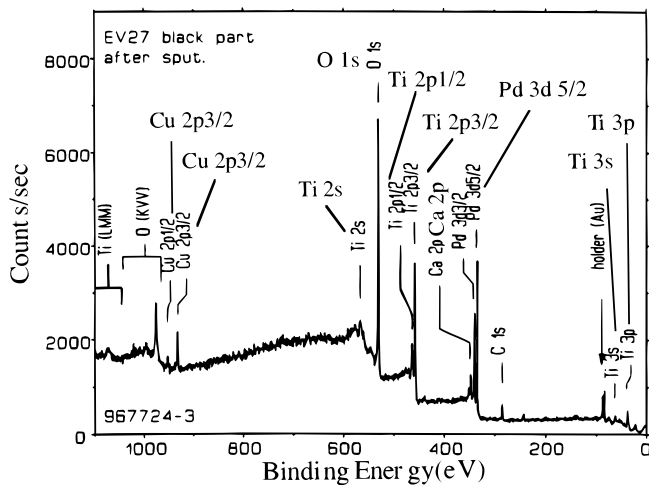
There are no instruments that can contaminate the Ti in the LiOD/D$_2$O solution. After the experiments, we keep the Pd samples in a desiccator in the clean room. The possibility of Ti being contaminated after an experiment is considered to be extremely low.

Another point to consider is that Ti atoms are not always detected. Sometimes, other elements are found, such as Si, Au, Pb, Cr, Cu, Fe, and so on; and sometimes, no elements except Pd are detected even though the experimental conditions are almost the same. In addition, the quantities of the detected elements vary. As is visible to the naked eye, the shades of the black circle are different every time; sometimes the circle corresponding to the shape of the Pt anode looks brown or metallic. We use the same experimental apparatus, solution and Pt anode, and Pd samples of the same batch of Tanaka Kikinzoku K.K. If these elements are deposited on the Pd surface by a certain contamination process, is it possible that the deposited elements and their quantities change?

In fact, the quantities of Au and Cu of EV34 seem larger than the others, and the impurities of EV36 are nearly equal to those of annealed Pd, according to Table II. The WDX spectra for the center surfaces of EV34 and EV36 are shown in Figs. 15 and 16. For EV34, peaks of Au and Cu can be noticed, whereas for EV36 only Fe and Pd peaks are noticed. These results can be realized by considering that Au and Cu exist on the surface of EV34. However, Au and Cu

many other impurities such as Pt or Cu are nearly equal to the concentrations of the other samples (as received, annealed, EV34, and EV36), why do only Ti atoms behave anomalously?

There is much more Pt than Ti because Pt is used as an anode and a Pd sample contains 200 μg/g. The concentration of Cu atoms is higher than Ti atoms, as can be seen in Table I. Why are Pt and Cu not concentrated on
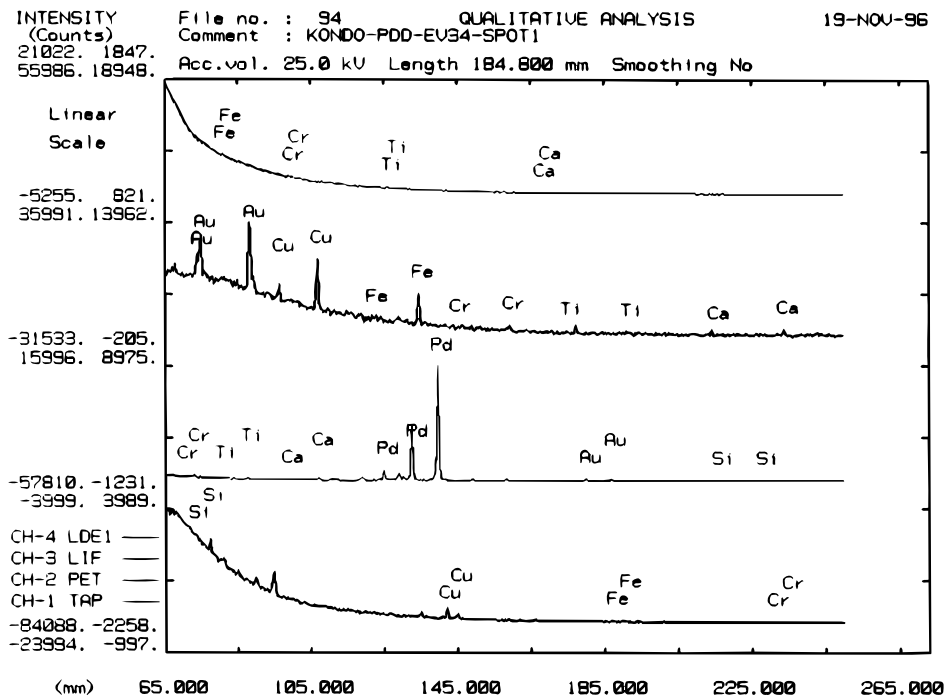

Fig. 15. The WDX spectrum of the EV34 spectrum (X-ray and neutron emission).

TABLE I

Impurity Analysis of LiOD/D_2O Solution and Pt Wire*

Ele-ments	Solution (μg/g)	Pt Wire (μg/g)	Ele-ments	Solution (μg/g)	Pt Wire (μg/g)	Ele-ments	Solution (μg/g)	Pt Wire (μg/g)
Li	———	C<0.5	Se	C<0.1	C<0.5	Eu	C<0.01	C<0.5
Be	C<0.01	C<0.5	Rb	C<0.01	C<0.5	Gd	C<0.01	C<0.5
B	10<C<100	C<1	Sr	0.01<C<0.1	C<0.5	Tb	C<0.01	C<0.5
Na	10<C<100	C<1	Y	C<0.01	C<0.5	Dy	C<0.01	C<0.5
Mg	0.01<C<0.1	0.5<C<1	Zr	0.01<C<0.1	C<0.5	Ho	C<0.01	C<0.5
Al	1<C<10	1<C<10	Nb	C<0.01	C<0.5	Er	C<0.01	C<0.5
Si	10<C<100	C<40	Mo	C<0.01	C<0.5	Tm	C<0.01	C<0.5
P	C<0.1	C<80	Ru	C<0.01	1<C<10	Yb	C<0.01	C<0.5
K	1<C<10	C<4	Rh	C<0.01	100<C<1000	Lu	C<0.01	C<0.5
Ca	0.1<C<1	1<C<10	Pd	C<0.01	10<C<100	Hf	C<0.01	C<0.5
Sc	C<0.01	C<0.5	Ag	C<0.01	1<C<10	Ta	C<0.01	C<0.5
Ti	C<0.01	C<3	Cd	C<0.01	C<0.5	W	C<0.01	C<0.5
V	C<0.01	C<3	In	C<0.01	C<0.5	Re	C<0.01	C<0.5
Cr	0.01<C<0.1	C<0.5	Sn	0.01<C<0.1	C<0.5	Ir	C<0.01	10<C<100
Mn	C<0.01	C<0.5	Sb	C<0.01	C<0.5	Pt	C<0.01	———
Fe	0.01<C<0.1	1<C<10	Te	C<0.01	C<0.5	Au	C<0.01	10<C<100
Co	C<0.01	C<0.5	Cs	C<0.01	C<0.5	Hg	C<0.01	C<0.5
Ni	C<0.01	C<0.5	Ba	0.1<C<1	C<0.5	Tl	C<0.01	C<0.5
Cu	0.01<C<0.1	1<C<10	La	C<0.01	C<0.5	Pb	C<0.01	1<C<10
Zn	C<0.01	C<0.5	Ce	C<0.01	C<0.5	Bi	C<0.01	C<0.5
Ga	C<0.01	C<0.5	Pr	C<0.01	C<0.5	Th	C<0.01	C<0.5
Ge	C<0.01	C<0.5	Nd	C<0.01	C<0.5	U	C<0.01	C<0.5
As	C<0.01	C<0.5	Sm	C<0.01	C<0.5			

*This LiOD solution(200ml) was exposed to experimental apparatus for 3 days without electrolysis.

can be sources of contamination (Au: a cooling pipe, which is coated by Au, and Cu: an electric terminal located on the top of the apparatus upper LiOD/D_2O solution). Although the possibility of contamination cannot be excluded in the case of Au and Cu, it is certain that elements on the surfaces of the Pd cathodes depend on an unspecified factor.

The last example of surface analysis is shown in Fig. 17. EV8 is the sample that emitted continuous long-term X rays. The elements Ca, Cr, Fe, Pt, Ti, and O are de-tected on the black circle on the surface of the electrolyte side. As these results indicate, a correlation between these elements detected on the Pd and nuclear products or ex-cess heat is not clear at present.

One problem is that we can observe only small spots ($\sim 10 \ \mu$m $\times 10 \ \mu$m) by EPMA, which we usually use in our laboratory. At present, we analyzed a few spots, and we assure that the results of the analysis are consistent. How-ever, it is better to analyze the total quantity by ICP mass.

TABLE II

ICP Mass Analysis of Pd Sample

Elements	Received (μg/g)	Annealed (μg/g)	EV27 (μg/g)	EV34 (μg/g)	EV36 (μg/g)
Ca	20	21	26	19	17
Ti	2.3	2.5	18	2.4	2.2
Cr	2.3	1.0	2.0	1.2	1.0
Fe	650	35	260	210	30
Ni	1.2	1.1	1.3	1.1	1.0
Cu	20	19	17	30	21
Pt	200	200	190	200	180
Au	5.7	5.6	4.9	7.5	5.3

The other problem is that some elements can be dissolved in the LiOD/D_2O solution. Because of this, we should analyze the solution after the experiment.

Another approach[7–9] is to observe isotope shifts of these elements detected on the Pd. It must be an effective way of considering the deposition mechanism of these elements. In any case, it is necessary to use several methods to investigate the origin of these elements on Pd electrodes.

Let us summarize the results and discussion of this section:

1. A Ti element of 21 μg (2.6×10^{17} atoms) was detected on the black circle of EV27.

2. The Ti element was confirmed by WDX, EDX, AES, XPS, and ICP-MS. The results are consistent with each other.

3. Considering the impurities contained in the experimental apparatus, one finds it difficult to assume that Ti is formed by any contamination process.

4. Other elements such as Ca, Cr, Fe, Cu, O, Au, or Pt were also detected, and the possibility of their being contaminants could not be excluded. However, if we assume that they are deposited by a certain contamination process, explaining the variation of the elements on Pd electrodes is difficult.

5. The correlation between the detected elements on the Pd electrodes and nuclear products or excess heat is not clear. Further investigation is needed by an improved method of analysis.

IV. CONSIDERATIONS ON REACTION MECHANISM

IV.A. Interpretation of Experimental Results by the EINR Model

According to our experimental results and the other many papers of this field, it is strongly suggested that certain nuclear reactions occur in the D_2-Pd system.
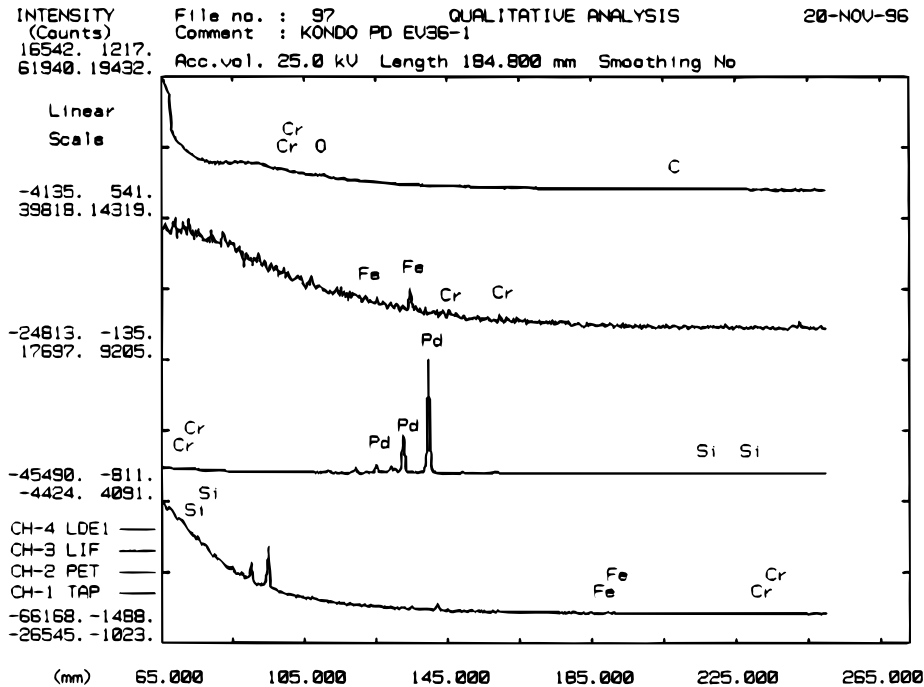

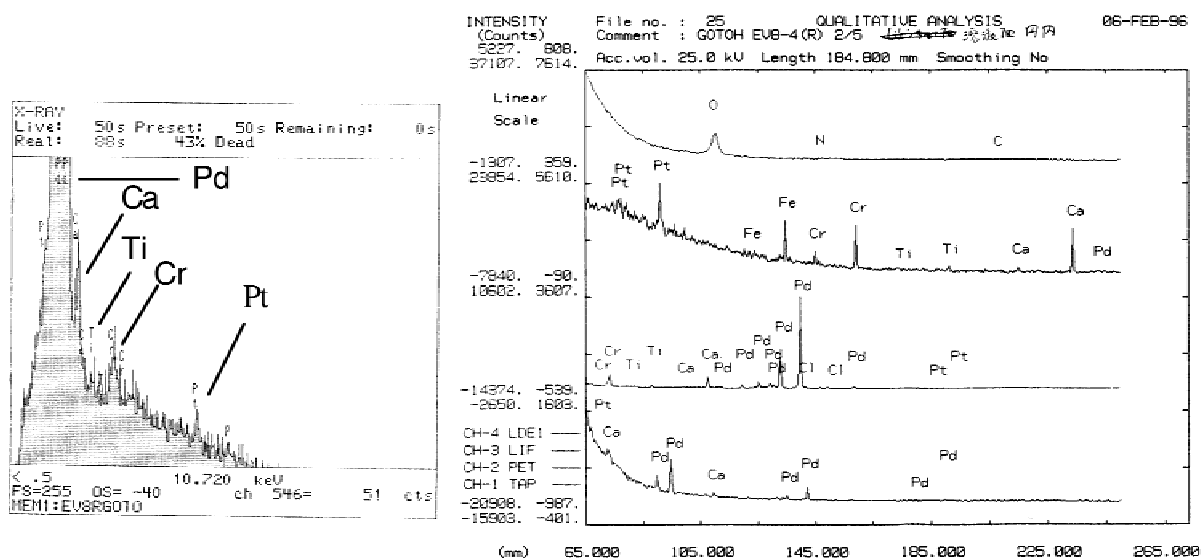Fig. 16. The WDX spectrum of the EV36 surface (no emission).

Fig. 17. The EDX and WDX spectra of the EV8 surface (long-term X-ray emission).

Chemical reactions cannot explain the X-ray and neutron emissions and the detection of the anomalous elements. Excess heat generation up to 10 keV/atom also cannot be produced by the known chemical reactions.

Then, what kind of nuclear reaction occurs? As is well known, D-D fusion was one of the candidates for explaining this phenomenon. However, at present, we can exclude the normal D-D fusion (D + D = p + T, D + D = n + ^{3}He) model for the following reasons:

1. The amount of excess heat is larger than the excess heat from nuclear products such as neutrons or tritium.

2. The emission rate of the neutrons is extremely low. Reproducibility of neutron emission is poor.

3. There is no clear correlation between neutron emissions and X-ray or excess heat generation.

From this discussion, we may say that D-D fusion cannot explain the phenomena; we may at least say that D-D fusion cannot play an important role.

What type of nuclear reaction could we assume? To discuss the reaction mechanism of the phenomena, we need to summarize our experimental results. Note that the following comments indicate just some aspects of the phenomena; experimental results depend on the experimental method and conditions such as the sensitivity limits of the detectors, the treatment of the Pd electrodes, or the applied current.

1. Titanium elements must be formed by certain nuclear reactions. Although it is not easy to introduce a new type of low-radiating nuclear reaction, it seems to be more difficult to use contamination to explain the obtained experimental results.

2. If Ti elements are formed by a new type of nuclear reaction, the detected elements such as Ca, Cr, Fe, Cu, or Au may also be synthesized by a similar nuclear process. However, note that the possibility of contamination is not completely excluded for these elements except Ti.

3. The detected X-ray spectrum looks continuous. If the continuous X ray was due to bremsstrahlung, one could consider that the X ray was generated by low-energy charged particles <100 keV.

4. The production rates of the neutrons, X rays, excess heat, and detected elements on the Pd electrodes are as follows:

Neutrons (n/s)	10 to 10^4
X rays (X ray/s)	10^2 to 10^4
Excess heat (event/s)	10^{12} (assuming that an event corresponds to few mega-electron-volts)
Ti (atom/s)	10^{12} (average rate: 2.6×10^{17} atoms/3.4×10^5/s)

These figures seem to suggest that Ti and excess heat are produced by primary nuclear reactions and neutrons and X rays are generated by secondary reactions.

5. The correlation between excess heat and nuclear products is unclear at present. Therefore, we may acknowledge the possibility that various and complicated nuclear reactions occur on the surface of Pd.

The foregoing discussions make it extremely difficult to understand the experimental results within the ordinary physicochemical knowledge. Therefore, we should introduce some hypotheses or a reaction model to explain the experimental results.

We introduce the EINR model. The outline of the model is as follows. If deuterons in Pd capture surrounding electrons, di-neutrons are formed. Then, the di-neutrons react to the surrounding nuclei and produce heat and other elements. Both nuclear reactions occur simultaneously.

One feature of the model is that electrons in deuterated Pd play important roles to trigger nuclear reactions. A second feature is that a neutron capture reaction chain produces anomalous elements on Pd electrodes.

Following facts provide the background for the model:

1. The existence of a di-neutron is accepted as a real substance in unstable nuclei such as ^{11}Li (Ref. 10).

2. An electron capture reaction is influenced by the states of orbital electrons; for example, the disintegration constant λ of the metal ^{7}Be is larger than that of BeF_2 (Ref. 11). The rate of orbital electron capture by a nucleus depends on the chemical bonding of the nucleus.

3. The cross section of the neutron capture reaction is large at low energies and small at high energies.

4. The deuteron has a weakly bonded nucleus. The binding energy of a deuteron is only 2.2 MeV.

Considering all the backgrounds, we propose the EINR model as one of the guiding models to investigate this new phenomenon. Needless to say, it is just an assumption to explain observed experimental results, which contain many problems to be solved and should be improved.

First, the electron capture by a deuteron occurs in deuterated Pd:

$$d + e^- \rightarrow {}^2n + \nu \ . \tag{8}$$

Simultaneously, further neutron capture reactions occur. In the following reactions, only exothermic nuclear reactions are assumed. Basically one di-neutron created at electron capture reacts with surrounding nucleus X, as expressed in the following equation:

$$X_Z^A + {}^2n \rightarrow X_Z^{A+2} \xrightarrow{\beta^-} Y_{Z+1}^{A+2} \ . \tag{9}$$
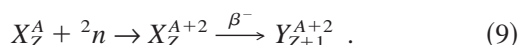
The tritium production reaction is an example of the equation, which is observed in our experiments[2,3,5]:

$$p + {}^2n \rightarrow t \xrightarrow{\beta^-} He_2^3 \ . \tag{10}$$

Helium-4 production, noticed as an important nuclear product, is also explained by this EINR model:

$$d + {}^2n \rightarrow H_1^4 \xrightarrow{\beta^-} He_2^4 \ . \tag{11}$$

It seems that a pair of di-neutrons also reacts with the surrounding nucleus. This type of reaction is expressed as follows:

$$X_Z^A + 2\,{}^2n \rightarrow X_Z^{A+4} \xrightarrow{\beta^-} Y_{Z+1}^{A+4} \xrightarrow{\beta^-} Z_{Z+2}^{A+4}(stable) \ . \tag{12}$$
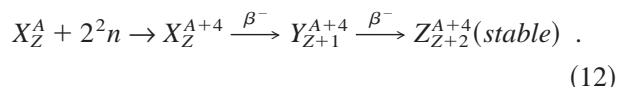
The elements Ti, Cr, and Fe detected on Pd can be explained in principle using the foregoing model as follows:

$$Ca_{20}^{44} + 2\,{}^2n \rightarrow Ca_{20}^{*48} \xrightarrow{\beta^-} Sc_{21}^{*48} \xrightarrow{\beta^-} Ti_{22}^{48} \tag{13}$$

$$Ti_{22}^{48} + 2\,{}^2n \rightarrow Ti_{22}^{*52} \xrightarrow{\beta^-} V_{23}^{*52} \xrightarrow{\beta^-} Cr_{24}^{52} \tag{14}$$

$$Cr_{24}^{52} + 2\,{}^2n \rightarrow Cr_{24}^{*56} \xrightarrow{\beta^-} Mn_{25}^{*56} \xrightarrow{\beta^-} Fe_{26}^{56} \ . \tag{15}$$
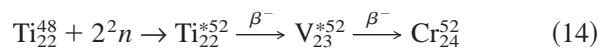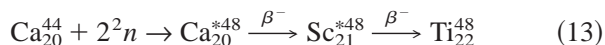
Calcium is selected as the origin of them. The Pd metal and D_2O/LiOD solution contain sufficient Ca, as shown in Tables I and II, to explain the elements obtained.

We assume that the conditions needed to cause the reaction are as follows:

1. a high concentration of deuterium

2. a high diffusion velocity of deuterium

3. the existence of a third element except Pd and deuterium.

Condition 1 means high D/Pd, which is widely recognized as an important factor in the field of cold fusion research. We demonstrate condition 2 in our previous papers. As to condition 3, it is experimentally shown that Ca is one of the third elements, as is described in Sec. IV.B.

Many problems should be solved using the EINR model. Both the stability of a di-neutron and a large enhancement of the cross section of the neutron capture are necessary. A certain mechanism for low-radiation transition from excited to bottom states of nuclei is also necessary. Nevertheless, it seems that the reactions of the participating electrons play an essential role in explaining the feature of the phenomenon: chemically affected nuclear reactions.

IV.B. Experimental Support of the EINR Model Using Multilayer Cathode (Pd/CaO/Pd)

The foregoing discussion reminds us of the following question: If enough Ca is given on the Pd surface, what will happen?

Figure 18 shows the structure of a multilayer cathode. The cathode was prepared by the following procedure. A Pd plate was etched with aqua regia (D_2O) to remove any impurity after washing by acetone and

Electrolyte Side

CaO/Pd
(1000Å, 3000Å)   Pd(400Å)
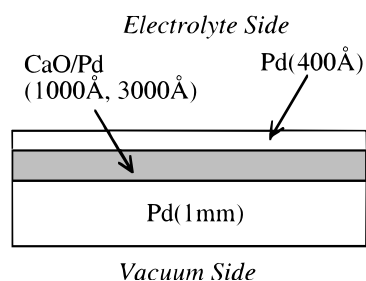
Pd(1mm)

Vacuum Side

Fig. 18. The structure of the multilayer cathode (Pd/CaO/Pd).

annealing, as described earlier. Enough annealing in a vacuum and sufficient etching with aqua regia (D_2O) cleans the surface of Pd. The sample was covered with a complex layer that consisted of CaO and Pd. It was formed by simultaneously sputtering of CaO and Pd with an Ar ion beam. The thickness of the layer was set from 1000 to 3000 Å. A thin Pd layer (400 Å) was formed on it by ion beam sputtering to prevent the dissolution of CaO into the D_2O/LiOD solution.

Features of the multilayer cathode are as follows:

1. The CaO/Pd complex layer is introduced to cause a nuclear reaction based on the EINR model.

2. The complex layer is put at the near surface of the electrolyte side because we assume that nuclear reactions occur at the near surface.

The experimental results using the multilayer cathodes are summarized in Table III. All the samples except EV56 belonged to the multilayer cathodes, although the thicknesses of the CaO/Pd layers were different. A thick Pd surface layer (1 μm) was chosen for EV56 so that no nuclear reactions might occur.

Both excess heat generation and X-ray emission were observed for all the multilayer cathodes, as shown in Table III. Maximum excess heat is shown in each column. Input power ranges from 20 to 40 W. X-ray emissions were simultaneously detected by X2 and X3 counters located at the upper side of the Pd. The maximum deviations from the mean values of X2 and X3 are shown in Table III. Neutron emission was observed only in the case of EV50; σ is the standard deviation of the background for each detector.

We observed excess heat generation and X-ray emissions for all the cases that we tried by using multilayer cathodes. It is suggested by our experimental results that Ca is one of the elements that can induce nuclear reactions. It is also suggested that Ca must exist at the near surface of Pd. These results are consistent with the EINR model in which Ca is the origin of nuclear reactions.

V. CONCLUDING REMARKS

We developed a new type of experimental apparatus to simultaneously measure excess heat and nuclear products to induce the continuous diffusion of deuterium.

TABLE III

Summary of Multilayer Cathode Experiments

Sample	Structure of Cathode	Excess Heat	X Ray	Neutron
EV50	Pd 400 Å CaO/Pd 1000 Å	Generation (maximum 3.2 W)	X1: Background X2,X3: Simultaneous detection X2($6.6\sigma_{X2}$), X3($6.2\sigma_{X3}$)	Burst $22\sigma_n$
EV51	Pd 400 Å CaO/Pd 3000 Å	Generation (maximum 1.5 W)	X1: Background X2,X3: Simultaneous detection X2($6.4\sigma_{X2}$), X3($7.8\sigma_{X3}$)	Background
EV52	Pd 400 Å CaO/Pd 1000 Å	Generation (maximum 1.9 W)	X1: Background X2,X3: Simultaneous detection X2($7.6\sigma_{X2}$), X3($8.8\sigma_{X3}$)	Background
EV53	Pd 400 Å CaO/Pd 3000 Å	Generation (maximum 1.8 W)	X1: Background X2,X3: Simultaneous detection X2($14.4\sigma_{X2}$), X3($16.6\sigma_{X3}$)	Background
EV56	Pd 1 μm CaO/Pd 1000 Å	None	X1,X2,X3: Background	Background
EV61	Pd 400 Å CaO/Pd 1000 Å	Generation (maximum 2.3 W)	X1: Background X2,X3: Simultaneous detection X2($6.4\sigma_{X2}$), X3($6.7\sigma_{X3}$)	Background

Continuous X rays ranging from 10 to 100 keV and neutron and excess heat production were observed. Titanium atoms were detected on the surface where deuterium atoms passed through on Pd cathodes after electrolysis. Quantitative discussion shows that the detected Ti atoms cannot be explained by contamination. An EINR model to explain the experimental results is introduced. Experimental support of the EINR model is shown by using a multilayer cathode containing Ca at the near surface of Pd. However, much work is needed to clarify this new phenomenon.

ACKNOWLEDGMENTS

REFERENCES

1. M. FLEISCHMANN and S. PONS, *J. Electroanal. Chem.*, **261**, 301 (1989).

2. Y. IWAMURA, T. ITOH, and I. TOYODA, "Observation of Anomalous Nuclear Effects in D$_2$-Pd System," *Trans. Fusion Technol.*, **26**, *4T*, Part 2, 160 (1994).

3. T. ITOH, Y. IWAMURA, N. GOTOH, and I. TOYODA, "Observation of Nuclear Products Under Vacuum Condition from Deuterated Palladium with High Loading Ratio," *Proc. 5th Int. Conf. Cold Fusion*, Monte Carlo, Monaco, April 9–13, 1995, p. 189.

4. T. ITOH, Y. IWAMURA, N. GOTOH, and I. TOYODA, "Observation of Nuclear Products in Gas Release Experiments with Electrochemically Deuterated Palladium," *Proc. 6th Int. Conf. Cold Fusion*, Toya, Japan, October 13–18, 1996, p. 410.

5. Y. IWAMURA, N. GOTOH, T. ITOH, and I. TOYODA, "Characteristic X-Ray and Neutron Emission from Electrochemically Deuterated Palladium," *Proc. 5th Int. Conf. Cold Fusion*, Monte Carlo, Monaco, April 9–13, 1995, p. 197.

6. Y. IWAMURA, N. GOTOH, T. ITOH, and I. TOYODA, "Correlation Between Behavior of Deuterium in Palladium and Occurrence of Nuclear Reactions Observed by Simultaneous Measurement of Excess Heat and Nuclear Products," *Proc. 6th Int. Conf. Cold Fusion*, Toya, Japan, October 13–18, 1996, p. 274.

7. T. MIZUNO et al., "Isotopic Distribution for the Elements Evolved in Palladium Cathode After Electrolysis in D$_2$O Solution," *Proc. Int. Conf. Cold Fusion*, Toya, Japan, October 13–18, 1996, p. 665.

8. T. OHMORI et al., "Production of Heavy Metal Elements and the Anomalous Surface Structure of the Electrode Produced During the Light Water Electrolysis on Au Electrode," *Proc. 6th Int. Conf. Cold Fusion*, Toya, Japan, October 13–18, 1996, p. 670.

9. G. H. MILEY et al., "Quantitative Observation of Transmutation Products Occurring in Thin-Film Coated Microspheres During Electrolysis," *Proc. 6th Int. Conf. Cold Fusion*, Toya, Japan, October 13–18, 1996, p. 679.

10. *Atomic and Nuclear Clusters*, G. S. ANAGNOSTATOS and W. VON OERTZEN, Eds., Springer-Verlag, New York (1994).

11. E. SEGRE, *Phys. Rev.*, **71**, 274 (1947).

Yasuhiro Iwamura (PhD, nuclear engineering, University of Tokyo, Japan, 1990) is a senior researcher at Advanced Technology Research Center (ATRC), Mitsubishi Heavy Industries, Ltd. He has a research background that includes electromagnetics on an accelerator for the fuel system of a tokamak, applied mathematics on an inverse problem, nuclear radiation measurement technology, and plasma chemistry. His current interests are in the area of low-energy nuclear reactions in solids and its application to industry.

Takehiko Itoh (MS, physics, Kyoto University Japan, 1989) is a researcher at ATRC. He has worked in the areas of optical properties in fine particles. His current research interests are in the area of nuclear reactions in solids.

Nobuaki Gotoh (BS, physics, Science University of Tokyo, Japan, 1988; MS, physics, Kyushu University, Japan, 1990; PhD, vacuum technology, The Graduate University for Advanced Studies, Japan, 1993) is a researcher at ATRC. He has studied three-body problems in nuclear physics and has worked in the areas of molecular science and vacuum technology.

Ichiro Toyoda (BS, physics, Science University of Tokyo, Japan 1980; MS, physics, Tohoku University, Japan, 1982) is a senior researcher at ATRC. He has worked in the areas of magnetochemistry, superconducting materials, and vacuum technology.